74th International Astronautical Congress (IAC), Baku, Azerbaijan, 2-6 October 2023.
Copyright ©2023 by Mr. Elliott Ruzicka. Published by the IAF, with permission and released to the IAF to publish in all forms.

IAC-23-C2.1.3

Morphology of Polyhedral Space Habitat Modules – Identifying the Ideal Form Using Multi-Criteria Analysis

Elliott Orion Ruzicka[a]

[a] *Orbital Design, 311 E 3rd Street, New York, NY, 10009, USA,* orion@orbital.design

Abstract

Over the past fifty years, the form and function of space habitat modules have remained largely unchanged. While cylindrical modules are relatively simple to transport and deploy, their limited size poses a challenge to their efficiency and usability. In contrast, large space habitat construction projects are costly and present logistical difficulties. The development of polyhedral modules could bridge the gap between these two approaches, allowing for modular, polyhedral units to be assembled and linked together to create larger habitats more efficiently and with less risk. However, identifying the most suitable polyhedron for use in space remains a critical question. Previous research has explored the construction of polyhedral modules, but little rigor has been applied to identifying the most optimal form. This is a crucial issue because the first module to be used will likely set the standard for subsequent modules and any disadvantages present at that time will be perpetuated. Therefore, it is essential to identify the optimal form prior to constructing prototypes. This research paper employs multi-criteria decision analysis and sensitivity analysis to compare various candidate polyhedra across several evaluation metrics, including number of faces, volume to surface area ratio, and joint stress, among several other quantitative and qualitative metrics. The results demonstrate that the Rhombic Dodecahedron is a particularly suitable candidate compared to other forms analyzed. Thus, the Rhombic Dodecahedron should be considered the standard polyhedral form for future research involving the development of polyhedral modules.

Keywords: space habitats, modular design, polyhedral modules, deployable structure, multi-criteria decision analysis, sensitivity analysis

Nomenclature

Variables

a	side length
ℓ	length
V	volume
A	area
R	ratio
T	tension
φ	dihedral angle
σ	stress
n	number
c	candidate polyhedrons
v	value

Subscripts

s	surface
a	apothem
i	importance levels
p	performance
n	normalized

Acronyms/Abbreviations

EVA	extra-vehicular activity
MCDA	multi-criteria decision analysis
GCR	galactic cosmic rays
SPE	solar particle event

1. Introduction

1.1 Prior Work by Others

Published in 1985, a paper by Frisina [1] described a framework for spaceframe construction that would allow for pressurized polyhedral volumes to be utilized and enlarged over time, and Frisina expanded this concept in a later 1994 paper [2]. This concept utilized extruded edge frames and isosceles triangular panels to create Isosceles Tetrahedra. This framework was notable in that it decouples the construction of the frame and the construction of the envelope. The isosceles triangles could be arranged in either a triangular frame or a square frame. It was also dimensionally rigid in stick frame form (in contrast to the Cube, for example). The author notes the importance of using space-filling polyhedra and the economy of utilizing a single face type.

In 2005, de Weck [3] published a paper proselytizing the virtues of the Truncated Octahedron as a spacecraft module form as opposed to the typical cylinder. Though de Weck notes the work of Frisina for recognizing the limitations of cylindrical module design, de Weck goes on to point out the infeasibility of using Irregular Tetrahedra as such for the construction of space habitat modules, citing the connections of necessarily fixed subsystems that would likely become critically interrupted with such a

Copyright ©2023 by Mr. Elliott Ruzicka. Published by the IAF, with permission and released to the IAF to publish in all forms.

framework. In de Weck's concept, the Truncated Octahedron modules would be launched into space in pre-assembled, limiting the final volume to what could fit inside a rocket fairing. While de Weck wrote extensively on the virtues of the Truncated Octahedron and briefly compared the Truncated Octahedron to the Cube, no other rigorous comparisons were attempted, despite mentioning other polyhedra such as the Tetrahedron, Octahedron, and Rhombic Dodecahedron.

Between 2018 and 2022, Ekblaw published several papers as well as a doctoral dissertation about the TESSERAE concept for self-assembling polyhedral modules [4,5,6,7,8,9,10]. This concept utilizes individual face units that can be stacked together and launched into space, and once in space can be assembled autonomously. This approach boasts a major advantage over de Weck's concept in that the pre-deployed panels can be stacked in a rocket fairing and then deployed into a much larger volume. While the early approach focused on the Truncated Icosahedron, Ekblaw later included the Truncated Octahedron, citing the work of de Weck and noting the virtues of space-filling polyhedra for large multi-module configurations.

1.2 Goal and Outline

The goal of this paper is to rigorously analyze several candidate polyhedra against an extensive list of evaluation metrics in order to determine, as close to objectively as possible, which candidate polyhedron is most ideal for use as a polyhedral space habitat module. For the purposes of this paper, a *space habitat* is a classification of space structure that can support and foster human life. Additionally, a *module* is a space structure that can be duplicated and connected to one another.

This paper will discuss which candidate polyhedra are included in the study and why, describe each evaluation metric used to compare the candidate polyhedra, explain the methodology for how the comparative analysis was conducted, and finally present the results of the analysis.

2. Candidate Polyhedra

While not all polyhedra can be included in this study, polyhedra that meet basic criteria should be included. The basic criteria for polyhedron inclusion are as follows:

(1) The line drawn from the center of each polyhedron face perpendicularly inwards should pass through the centroid of the polyhedron. This includes all polyhedra that can perfectly be inscribed with a sphere. In other words, each face should be tangent to an in-sphere.

(2) Candidate polyhedrons should be selected from the simpler end of the spectrum of polyhedra moving toward more complex. The shorthand for this criterion was face-count.

(3) The number of polyhedrons was intentionally limited for reasons of practicality. While somewhat arbitrary, this number was set to (10).

(4) Preference was given to space filling polyhedrons and those that have been studied in prior research.

For the final criterion, the Triangular Prism and Hexagonal Prism were chosen for their space filling property, the Truncated Icosahedron was selected for its preference in the work of Ekblaw [4,5,6,7,8,9,10], and the Truncated Octahedron was selected for its preference in the works of both Ekblaw [5,7,8] and de Weck [3].

2.1 Candidate Descriptions

This section contains brief descriptions of the candidate polyhedrons as well as a symbol between brackets for quick reference throughout (see Fig. 1).

2.1.1 Tetrahedron {T}

Platonic solid comprised of (4) equilateral triangles.

2.1.2 Cube {C}

Space filling Platonic solid comprised of (6) squares.

2.1.3 Octahedron {O}

Platonic solid comprised of (8) equilateral triangles.

2.1.4 Dodecahedron {D}

Platonic solid comprised of (12) regular pentagons.

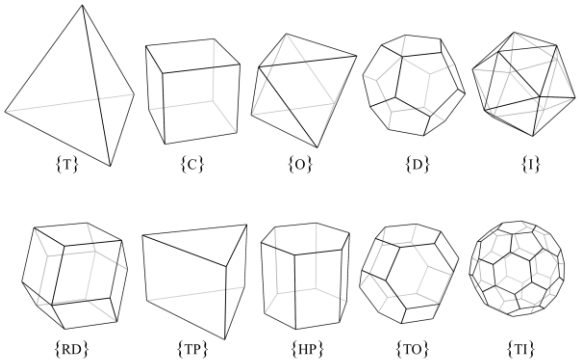

Fig. 1. Candidate polyhedra

Copyright ©2023 by Mr. Elliott Ruzicka. Published by the IAF, with permission and released to the IAF to publish in all forms.

2.1.5 Icosahedron {I}

Platonic solid comprised of (20) equilateral triangles.

2.1.6 Rhombic Dodecahedron {RD}

Space filling Catalan solid comprised of (12) rhombi, each with a diagonal ratio of $1 : \sqrt{2}$.

2.1.7 Triangular Prism {TP}

Space filling prism comprised of (2) equilateral triangles and (3) oblong rectangles, each with a proportional ratio $a{:}\ell$ of $1{:}1/\sqrt{3}$, where a is the side length of the equilateral triangle and ℓ is the extruded length of the prism*.

2.1.8 Hexagonal Prism {HP}

Space filling prism comprised of (2) regular hexagons and (6) oblong rectangles, each with a proportional ratio $a{:}\ell$ of $1{:}\sqrt{3}$, where a is the side length of the regular hexagon and ℓ is the extruded length of the prism*.

2.1.9 Truncated Octahedron {TO}

Space filling Archimedean solid comprised of (8) regular hexagons and (4) squares.

2.1.10 Truncated Icosahedron {TI}

Archimedean solid comprised of (20) regular hexagons and (12) regular pentagons.

3. Evaluation Metrics

For this study, (14) comparison metrics were chosen, each having a meaningful bearing on a given polyhedron's suitability for use in space. This list was compiled from a larger list of potential metrics and pared down to this number (for reasons explained in the section Comparison Methodologies) based on their importance and the degree to which these metrics could be compared on a linear scale or as a Boolean.

Each evaluation metric should be considered in isolation. That is to say, while a given metric may correlate with another metric (ex: Number of Faces and Volume to Surface Area Ratio), each metric should be judged on its own merits in order to avoid bias in metric selection. The following is a list of the evaluation metrics used in this study with no order of importance implied.

- Number of Faces
- Number of Face Types
- Number of Edges
- Volume to Surface Area Ratio
- Deployed Volume Larger than Stowage Volume
- Face Apothem Similarity
- Face Tension
- Joint Stress
- Simulated Stress
- Space-Filling
- Number of Face-Connected Modules
- Lattice-Forming
- Unfolding Deployability
- Fit in Rocket Fairing

3.1 Virtue Categories

Each of the evaluation metrics chosen for analysis represent at least one of the following virtue categories in space design: simplicity, economy, structure, functionality, practicality. Note that a given evaluation metric may appear in more than one category.

3.1.1 Simplicity
- Number of Faces
- Number of Face Types
- Number of Edges

3.1.2 Economy
- Number of Face Types
- Number of Edges
- Volume to Surface Area Ratio
- Deployed Volume Larger than Stowage Volume

3.1.3 Structure
- Number of Face Types
- Face Tension
- Joint Stress
- Simulated Stress
- Space Filling

3.1.4 Functionality
- Space Filling
- Number of Face-Connected Modules
- Face Apothem Similarity
- Lattice-Forming

3.1.5 Practicality
- Number of Faces
- Unfolding Deployability
- Fit in Rocket Fairing

3.2 Individual Metrics

3.2.1 Number of Faces

3.2.1.1 Reasoning

In the context of polyhedral space habitat modules, a polyhedron with a lower number of faces

* This proportion of side length a to length ℓ was selected as it maximizes the volume : surface area ratio.

Copyright ©2023 by Mr. Elliott Ruzicka. Published by the IAF, with permission and released to the IAF to publish in all forms.

holds greater appeal compared to a polyhedron with many faces.

During the construction process, a polyhedral space habitat module with fewer faces significantly mitigates assembly complexity, expedites the assembly time, and reduces the likelihood of encountering single-point assembly failures.

For reconfigurable polyhedral habitats, wherein integrated systems are embedded within each face panel, having more faces entails a proportional increase in redundant integrated systems. Consequently, this escalation in redundant systems constitutes inefficiencies, more single-point failures, and potential complications in the overall functioning of the habitat.

Once the module is fully assembled and operational, the face panels must exchange utilities with their neighbors. Basic utilities such as electricity, data, coolant, and water must be efficiently transferred between face panels to allow for utility distribution within and without a module. In this regard, polyhedral configurations with a higher number of faces impose a higher demand for utilities to be routed across a greater number of interfaces, thereby increasing the likelihood of misalignment and choke point failures.

3.2.1.2 Raw Value Methodology

The number of faces for each polyhedron is a known attribute. The raw value for this metric is the number of faces.

Table 1. Number of Faces raw values

{T}	{C}	{O}	{D}	{I}	{RD}	{TP}	{HP}	{TO}	{TI}
4	6	8	12	20	12	5	8	14	32

3.2.2 Number of Face Types

3.2.2.1 Reasoning

The number of face types within a particular polyhedron directly affects the design efficiency of a polyhedral space habitat module. Minimizing the variety of face types within the module is advantageous, with a preference for a single face type ideally.

Employing a single face type in the module design leads to notable cost savings in various aspects of the project. By limiting the face types to one, the requirements for design, engineering, fabrication, and qualification testing can be minimized, streamlining the overall development process. In contrast, introducing multiple face types necessitates allocating additional resources for face-specific design, engineering, fabrication, and qualification testing, which consequently escalates the overall project cost.

The adoption of a single face type ensures the interchangeability of all panels within the habitat module. This inherent uniformity allows any panel to be used interchangeably and in any other position, facilitating ease of assembly, maintenance, and repair operations. In contrast, employing more than one face type compromises this interchangeability.

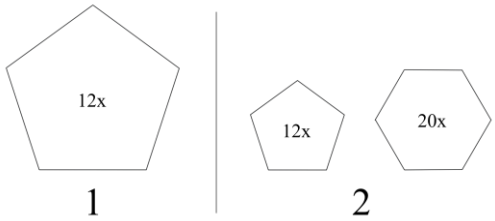

Fig. 2. Number of face types for {D} (left) and {TI} (right)

3.2.2.2 Raw Value Methodology

The number of face types for each polyhedron is a known attribute (see Fig. 2). The raw value for this metric is the number of distinct types of faces.

Table 2. Number of Face Types raw values

{T}	{C}	{O}	{D}	{I}	{RD}	{TP}	{HP}	{TO}	{TI}
1	1	1	1	1	1	2	2	2	2

3.2.3 Number of Edges

3.2.3.1 Reasoning

An increase in the number of edges of a polyhedral module yields several significant implications, particularly pertaining to structure and utility management.

The edges of an internally pressurized polyhedron module with pinned faces are structural weak points. While the stress can be carried along the larger cross section of the faces, these stresses are concentrated at the joints, necessarily rendering them weak points. All things being equal, weak points should be reduced as much as possible.

For the module to retain pressure, the edges must function as seals, presumably gaskets if the panels are to be reconfigurable. A higher number of edges means a higher number of gaskets and thereby a higher likelihood of possible leakages. While not completely a linear relationship, more edges is roughly correlated to a greater total edge length, and consequently a greater total length of gaskets, which increases the potential leakage points.

A higher number of edges increases the opportunities for misfits in both structural, gasket, and utility connections. As the complexity of the module increases with a higher number of edges, ensuring

Copyright ©2023 by Mr. Elliott Ruzicka. Published by the IAF, with permission and released to the IAF to publish in all forms.

precise alignment during the assembly processes becomes more challenging.

3.2.3.2 Raw Value Methodology

The number of edges for each polyhedron is a known attribute. The raw value for this metric is the number of edges.

Table 3. Number of Edges raw values

{T}	{C}	{O}	{D}	{I}	{RD}	{TP}	{HP}	{TO}	{TI}
6	12	12	30	30	24	9	18	26	90

3.2.4 Volume to Surface Area Ratio

3.2.4.1 Reasoning

The volume to surface area ratio is a crucial metric with significant economic implications when designing space habitat modules. A higher volume to surface area ratio is economically advantageous.

The main economic argument for favoring a high volume to surface area ratio is the relationship between surface area and mass. As the surface area of a unit volume increases, the mass of the module also increases as the face panels constitute the mass of the empty module. Mass-to-orbit is one of the fundamental considerations when launching orbital modules. Higher mass requires more significant propulsion capabilities and fuel expenditure during launch, contributing to increased launch costs. While the launch cost savings are not necessarily linear (as the actual savings depend greatly on the architecture and variety of available launch vehicles [11]), all things being equal, lowering mass reduces the launch costs.

3.2.4.2 Raw Value Methodology

Given a unit volume of 1, the surface areas for all studied polyhedrons were found using the volume and surface area formulas.

1. Using the appropriate volume equation (see appendix) and input V=1, find the side length a.

2. Using the appropriate surface area equation (see appendix) and input a, find the surface area A_s.

3. For each polyhedron, the volume to surface area ratio is given by dividing the unit volume of 1 by the surface area.

$$R = \frac{V}{A_S} \quad (1)$$

The raw value for this metric is the ratio R found in step 3.

Table 4. Volume to Surface Area raw values

{T}	{C}	{O}	{D}	{I}	{RD}	{TP}	{HP}	{TO}	{TI}
0.139	0.167	0.175	0.188	0.194	0.187	0.153	0.175	0.188	0.200

3.2.5 Deployed Volume Larger than Stowage Volume

3.2.5.1 Reasoning

A deployable module should never be smaller than the cylindrical space occupied while stowed in the fairing. In cases where the deployed dimensions are smaller, the advantages of on-orbit assembly are negated, as the fully assembled module would essentially occupy the same (or less) volume as its stowed configuration (see Fig 3). This scenario would bestow negative value on the on-orbit assembly process when compared to launching a pre-assembled module with the same volume as its stowage area.

For the purposes of this analysis, the internal fairing dimensions of a SpaceX Falcon 9 rocket fairing were used (4.57m diameter, 11.5m length) [12], as it is currently among the highest capacities and mass-to-orbit capabilities at the time of publication with a long track record of successful launches. See also section 3.2.14.

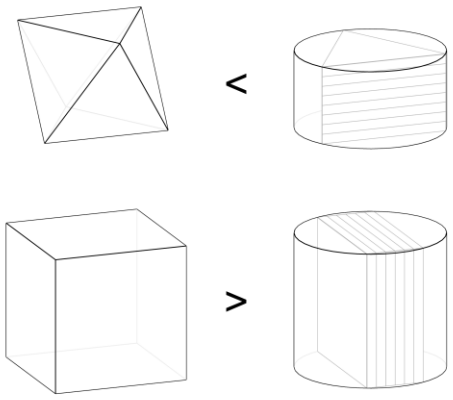

Fig. 3. Examples showing deployed volume smaller than stowage volume {O} and deployed volume larger than stowage volume {C}

3.2.5.2 Raw Value Methodology

There are two simple methods for stowing the individual face panels in a cylindrical rocket fairing: (1) stacked parallel to the main axis of the fairing and (2) stacked perpendicular to the main axis of the fairing. For each method and for each polyhedron, the max panel size was fit inside the model fairing size using trigonometric formulas for the panel shape and a notional panel thickness*. The deployed volume for

* This notional panel thickness was set to 0.3m for all calculations (see section 6.2.3).

Copyright ©2023 by Mr. Elliott Ruzicka. Published by the IAF, with permission and released to the IAF to publish in all forms.

the polyhedron is found using the side length *a* of the panel and the polyhedron's volume equation. The stowage volume is found by taking the area of the notional fairing cross-section and multiplying it by the axial length of the stowed panels.

If the deployed volume is larger than the stowage volume for either packing method, then the metric is considered satisfied. The raw value of this metric is a Boolean, reading as 1 for polyhedra that have a deployed volume larger than the stowage volume and 0 for polyhedra that don't.

Table 5. Deployed Volume Larger than Stowage Volume raw values

{T}	{C}	{O}	{D}	{I}	{RD}	{TP}	{HP}	{TO}	{TI}
0	1	0	1	1	1	0	1	1	1

3.2.6 Face Apothem Similarity

3.2.6.1 Reasoning

The face apothem, defined as the distance between the face centroid and the nearest edge of a shape, serves as a critical parameter influencing the available space within each face panel for accommodating contiguous systems or modular panel inserts (see Fig. 4).

To ensure the full utilization of each panel and achieve functional equivalence, it is advantageous for all panels to have similar apothem dimensions. Panels with more-similar apothem dimensions can readily accommodate comparable magnitude and forms of integrated systems, rendering them equally functional and versatile. This uniformity in apothem dimensions allows for standardized integration of systems and components, simplifying the design, engineering, and assembly processes across all panels.

Ideally, if each panel possesses the same apothem dimensions, it indicates that all panels are of the same shape, achieving perfect functional equivalence.

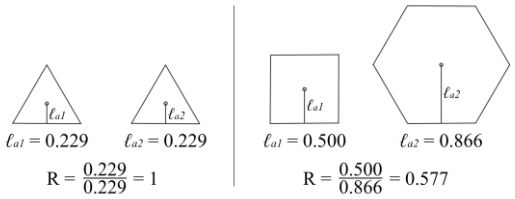

Fig. 4. Face apothems and ratios of {I} (left) and {TO} (right)

3.2.6.2 Raw Value Methodology

For each face type of each polyhedron of a unit volume, the apothem is given by using the appropriate formula for the polygon in question (see appendix).

For each apothem length, the smaller value is divided by the larger value to arrive at a ratio. For polyhedrons with a single face type, this ratio will equal 1. The raw value for this metric is the aforementioned ratio in decimal form.

Table 6. Face Apothem Similarity raw values

{T}	{C}	{O}	{D}	{I}	{RD}	{TP}	{HP}	{TO}	{TI}
1	1	1	1	1	1	1	0.577	0.577	0.795

3.2.7 Face Tension

3.2.7.1 Reasoning

The maximum tension experienced by a uniformly loaded panel is influenced by the uniform pressure load, the dihedral angle, and the apothem length. This tension can be seen in the vector diagrams (see Joint Force). Longer apothem lengths and larger dihedral angles result in higher maximum face tension, requiring more structure to resist this tension. Since more structure contributes more weight and/or volume, this acts against the goals of reducing mass and increasing internal volume.

3.2.7.2 Raw Value Methodology

For each polyhedron:

1. Using the appropriate volume equation (see appendix) and input V=1, find the side length a.
2. Using the appropriate trigonometric formulas, find the apothem length ℓ_a.
3. The tension T can be found using the following equation:

$$T = \frac{\ell_a}{tan(90 - (\frac{\varphi}{2}))} \quad (2)$$

The raw value for this metric is the tension value T found in step 3.

Table 7. Face Tension raw values

{T}	{C}	{O}	{D}	{I}	{RD}	{TP}	{HP}	{TO}	{TI}
0.416	0.500	0.523	0.565	0.584	0.561	0.458	0.525	0.743	0.672

3.2.8 Joint Stress

3.2.8.1 Reasoning

Joint stress results from the transmission of pressure along the face of each panel until it reaches the edge, where it is transmitted into the smaller cross section of the joint. This is an important consideration in any pressurized structure.

Similar to face tension, the maximum stress experienced by the joint is influenced by the following factors: the magnitude of the uniform pressure load, the shape and size of the adjacent

Copyright ©2023 by Mr. Elliott Ruzicka. Published by the IAF, with permission and released to the IAF to publish in all forms.

panels (characterized by the apothem lengths), and the dihedral angle. For a given internal pressure (ex: 14 psi), the load builds up along the panel face until reaching the edge where that load is resolved by the joint through stress and the panel face through tension. Each joint must resist the pressure load of each adjacent panel, and the panels must resolve the outward force at the joints through tension. The result of these forces can be shown geometrically using vector diagrams (see Fig. 5). These force vector diagrams show that the stress on the joints will always be higher (and more concentrated) than those in the face panels. For a given volume, minimum joint stresses are achieved when the panel face size is balanced against the dihedral angle.

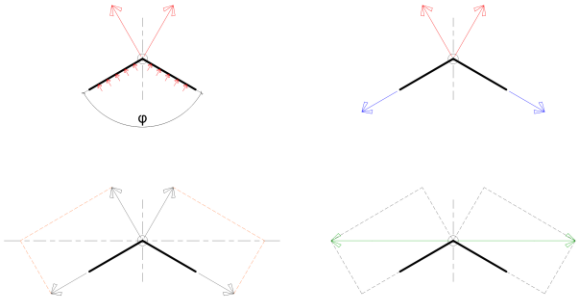

Fig. 5. Diagram of forces; a) uniform distributed pressure load and resultant magnitude of reaction forces on the joint (red); b) magnitude of reaction forces (red) balanced by the magnitude of face tension (blue); c) line of action of net force vectors (orange); d) magnitude of opposing forces on the joint (green)

3.2.8.2 Raw Value Methodology

For each polyhedron:

1. Using the appropriate volume equation (see appendix) and input V=1, find the side length a.

2. Using the appropriate trigonometric formulas, find the apothem length ℓ_a (see appendix).

3. The joint stress can be found using the following equation:

$$\sigma = \frac{\ell_a}{cos(90 - (\frac{\varphi}{2}))} \quad (3)$$

The raw value for this metric is the stress value φ found in step 3.

Table 8. Joint Stress raw values

{T}	{C}	{O}	{D}	{I}	{RD}	{TP}	{HP}	{TO}	{TI}
0.721	0.707	0.641	0.665	0.625	0.647	0.684	0.742	0.667	0.710

3.2.9 Simulated Stress

3.2.9.1 Reasoning

Whole-system simulations of polyhedral space habitat modules is important to consider due to the combined effects of face stress and joint stress, the combination of which may not be accurately predicted when analyzed in isolation.

In a comprehensive whole-system simulation, both face stress and joint stress interact and influence each other in complex ways. The stress distribution within the module is affected by the interconnectedness of faces and joints, leading to stress concentrations at specific locations that cannot be anticipated solely through separate face and joint simulations.

To ensure a comprehensive and accurate assessment of the structural integrity, it is prudent to conduct simulations under internally pressurized conditions for each candidate polyhedron. By examining the maximum stresses experienced within the polyhedron, both face stress and joint stress can be accounted for, offering a more realistic representation of the module's structural performance.

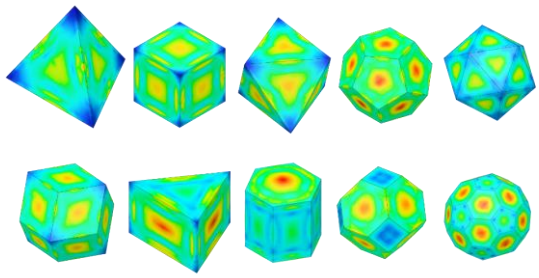

Fig. 6. Stress simulations, independent color coding

3.2.9.2 Raw Value Methodology

Each polyhedron was modelled in Fusion 360, each with a total exterior volume of 216m^{3*} and each with a faceted shell thickness of 0.3m. The polyhedrons were modelled as hollow solids, which has the joints acting as moment connections as opposed to pinned connections. Future analysis should account for pinned connections as this would more accurately represent the general joint condition.

The interior faces of the models were loaded with 14 psi and the simulation was run (see Fig. 6). The raw value for this metric is the maximum stress output by the simulation for each candidate polyhedron.

* For the purposes real-world practicality, a maximum practical volume of habitat was decided to be 216m^3, which can be visualized as a cube 6 meters to an edge (see section 6.2.3).

Copyright ©2023 by Mr. Elliott Ruzicka. Published by the IAF, with permission and released to the IAF to publish in all forms.

Table 9. Simulated Stress raw values

{T}	{C}	{O}	{D}	{I}	{RD}	{TP}	{HP}	{TO}	{TI}
9.393	6.406	3.633	2.690	2.048	2.873	6.688	5.363	3.571	1.484

3.2.10 Space-Filling

3.2.10.1 Reasoning

The space-filling attribute holds significant advantages in the design of polyhedral space habitat modules, enhancing the overall performance of the habitat in the domains of functionality, safety, structure, and shielding. A polyhedron is considered space-filling if multiple copies of the polyhedron can completely tile 3D space, leaving no gaps in between the modules.

Space-filling modules allow for the complete utilization of space across the total size of an agglomeration of modules.

The numerous connection possibilities between space-filling modules offer unparalleled order, hierarchy, and flexibility in designing and customizing the habitat layout and circulation paradigm when compared to modules that cannot fill space.

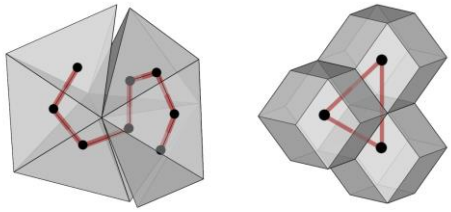

Fig. 7. Non-looping and looping modules

Additionally, the space-filling characteristic ensures the creation of looping pathways throughout the habitat. The availability of looping pathways allows for efficient navigation and evacuation routes during critical situations, thereby eliminating the possibility of dead-end corridors and improving emergency safety (see Fig. 7). It is important to note that while space-filling polyhedra are not required for forming looping pathways, all space-filling polyhedra do possess this advantageous property. For example, the Truncated Icosahedron can form looping pathways despite not being space-filling (see section 3.2.12 - Lattice-Forming).

Moreover, space-filling modules present unique opportunities for creating enclosed volumes in-between modules. By tiling modules in such a way that they completely surround an empty volume of space, this space can be considered "free volume" (see Fig. 8). It can be used as secure vacuum storage, EVA training space, or even usable volume for instruments or equipment that do not require an atmosphere. Provided that the face panels can accommodate the extra load (either through over-design or supplementary structural members), this enclosed volume can even be pressurized (provided that the panel joints are adequately sealed and protected). This new pressurized volume can be as small as a single module or even many times larger provided that the structural support is adequate.

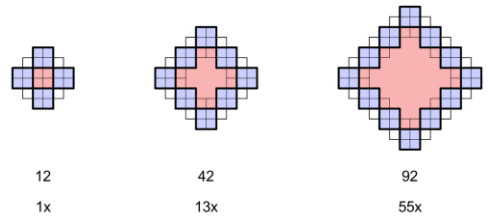

Fig. 8. Multiple {RD} modules enclosing space, showing the total modules used and the enclosed volume

A structural advantage of space-filling modules is their ability to create a more rigid and stable conglomerated structure. By utilizing space-filling polyhedra, each module can distribute eccentric forces between neighboring modules more effectively, leading to a more robust and interconnected structural system. This structural integrity is particularly crucial in the demanding environment of space, where the habitat must withstand various external forces experienced during docking, berthing, acceleration, and any other events that may cause non-uniform live loads and eccentric loads.

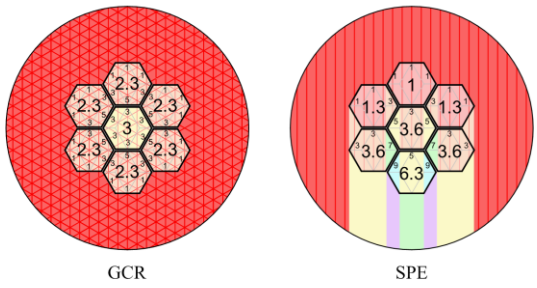

Fig. 9. Diagram of module layers cumulatively adding protection from radiation due to GCR and SPE

Furthermore, by maximizing the usable volume within the agglomeration, the face panels of space-filling polyhedra can more effectively and predictably act as radiation shielding for successive interior layers, and the overall radiation exposure area is minimized (see Fig. 9). In the event of a SPE, occupants can increase their protection by retreating

Copyright ©2023 by Mr. Elliott Ruzicka. Published by the IAF, with permission and released to the IAF to publish in all forms.

to the interior modules of a larger conglomeration of modules.

3.2.10.2 Raw Value Methodology

Space-filling ability is a known attribute. The raw value for this metric is a Boolean, reading as 1 for space-filling polyhedra and 0 for non-space-filling polyhedra.

Table 10. Space-Filling raw values

{T}	{C}	{O}	{D}	{I}	{RD}	{TP}	{HP}	{TO}	{TI}
0	1	0	0	0	1	1	1	1	0

3.2.11 Number of Face-Connected Modules

3.2.11.1 Reasoning

Each module will be able to connect to one or more other modules via a face-face connection. The number of modules a given module will be able to connect to depends on the shape of the module. A higher number of connection opportunities between modules results in an increased number of different spaces that can be accessed from any given module. This enhanced connectivity significantly improves the overall flexibility and functionality of the habitat, reducing travel time and fostering collaboration (see Fig. 10).

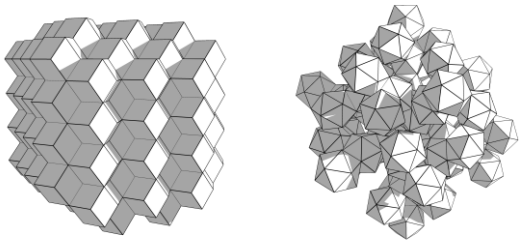

Fig. 10. Conglomeration of {RD} (left) and {I} (right)

3.2.11.2 Raw Value Methodology

For the maximum condition, the number can be determined by taking a single polyhedron of each type and attempting to cover each of its faces with other copies of itself by mirroring the original over said faces. For many polyhedrons, this will be possible for all faces without overlapping and the maximum figure will equal the number of faces of that polyhedron, but for some polyhedra the copies will get in the way of further copies and the average number of connections will be less than the maximum number. For each polyhedron, connected modules were added by face-mirroring, attempting to maximize the number of connections. This was conducted for three generations of mirroring, and the average number of connections was recorded for the second generation. This average value is the raw value for this metric.

Table 11. Number of Face-Connected Modules raw values

{T}	{C}	{O}	{D}	{I}	{RD}	{TP}	{HP}	{TO}	{TI}
3.333	6	2.9	2.313	2.5	12	5	8	14	6

3.2.12 Lattice-Forming

3.2.12.1 Reasoning

When connected in a large formation, a lattice is formed when the modules connect in a regular, repeating pattern across three dimensions, also known as tessellation.

One key advantage of the lattice formation is the ability to create looping circulation pathways within the space habitat. These looping pathways are crucial for ensuring safe egress to a secure location during emergencies. By avoiding dead-end corridors, occupants can efficiently navigate through the habitat and swiftly evacuate to safety when necessary. This attribute is particularly vital in the space environment, where emergency situations may arise and require rapid and unimpeded movement to other areas, as emergency EVA egress is unlikely.

Additionally, the lattice formation facilitates wayfinding in large agglomerations of modules. The interconnected lattice structure provides clear and well-defined pathways, reducing the likelihood of getting disoriented or lost within the habitat. This ease of navigation contributes to a more intuitive living and working environment for the occupants.

Furthermore, the lattice formation creates a robust super-structure that enhances the overall structural integrity of the space habitat (see Fig. 11). The lattice's interconnected network distributes loads and forces more effectively, reducing stress concentrations and increasing the module's resistance to external forces. This added structural strength improves the habitat's stability and longevity in the harsh conditions of space.

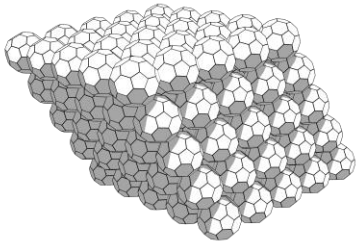

Fig. 11. A lattice of {TI}

Copyright ©2023 by Mr. Elliott Ruzicka. Published by the IAF, with permission and released to the IAF to publish in all forms.

3.2.12.2 Raw Value Methodology

Lattice-forming ability is a known attribute. The raw value for this metric is a Boolean, reading as 1 for lattice forming polyhedra and 0 for non-lattice forming polyhedra.

Table 12. Number of Face-Connected Modules raw values

{T}	{C}	{O}	{D}	{I}	{RD}	{TP}	{HP}	{TO}	{TI}
0	1	0	0	0	1	1	1	1	1

3.2.13 Unfolding Deployability

3.2.13.1 Reasoning

Deployability by unfolding holds several advantages over individual assembly for space habitat modules.

One key advantage of serial, unfolding deployability is the efficiency it offers during deployment. The habitat module can be stacked together as a single unit, with each face panel connected on one edge to the next face panel in the stack. The face panels can then be unfolded, one panel at a time, without losing or damaging the panels, until achieving the final polyhedral form. This eliminates the risk of losing individual panels during assembly and precludes the necessity for a large container that keeps all the panels from floating away accidentally [4,5,6,8,9].

Moreover, unfolding deployability reduces the reliance on complicated software or individual guidance systems during the initial deployment [4,5,6,7,8,9]. While propulsion and guidance systems could still be used for fine-tuning or reconfiguration, the primary deployment mechanism relies only on stored energy systems within the unfolding module. This design approach minimizes the need for complex and potentially failure-prone software or guidance systems during the crucial deployment phase. Stored energy systems, such as springs, elastic materials, or shape memory materials can be employed to economically actuate the folding deployment. These energy storage mechanisms allow the module to be compactly stowed during launch and then self-deploy upon reaching its intended destination. The utilization of such energy storage systems reduces mass and complexity.

3.2.13.2 Raw Value Methodology

This is a metric that requires individual investigation in order to determine qualification, however polyhedra with more than one face type universally do not qualify. If all the face panels can be stacked face to face, and then unfolded one joint at a time with no collisions until resulting in the completely deployed module, the quality of folding deployability applies.

The raw value for this metric is a Boolean, reading as 1 for polyhedra that can be deployed via unfolding and 0 for polyhedra that cannot.

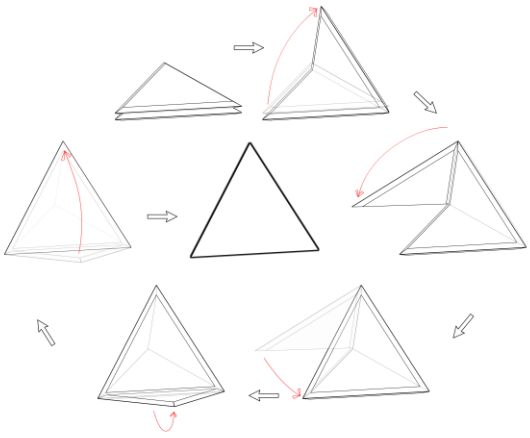

Fig. 12. Unfolding deployment of {T} module

Table 13. Unfolding Deployability raw values

{T}	{C}	{O}	{D}	{I}	{RD}	{TP}	{HP}	{TO}	{TI}
1	1	1	1	1	1	0	0	0	0

3.2.14 Fit in Rocket Fairing

3.2.14.1 Reasoning

To ensure the practicality and timely employment of a polyhedral space habitat module concept, it is highly advantageous for the module's pre-deployment dimensions to be compatible with the fairing size of currently in-service rockets. This metric assesses whether a deployed polyhedral module with a volume of 216m^3 can fit into the model fairing volume in its pre-deployed state.

If the polyhedral module concept were employed, it would be ideal for the module's shape to be compatible with existing rocket fairings. Waiting for future increased capacity in rocket fairings would necessarily introduce uncertainty and delays in launching the space habitat module. Furthermore, retrofitting or modifying current fairings to accommodate larger modules may involve significant costs and technical challenges.

By adhering to the dimensions of currently in-service rocket fairings, the polyhedral space habitat module can be readily launched using existing launch vehicles, streamlining the deployment process and accelerating the realization of polyhedral space habitat modules.

Copyright ©2023 by Mr. Elliott Ruzicka. Published by the IAF, with permission and released to the IAF to publish in all forms.

3.2.14.2 Raw Value Methodology

For each polyhedron:

1. Assuming a volume of 216m^3 and a panel thickness of 0.3m, find the panel dimensions.
2. Determine the size that the panels occupy in the most advantageous configuration.
3. If the outer dimensions of the stacked panels are smaller than the notional fairing dimensions, then the polyhedron meets the metric criteria.

The raw value of this metric is a Boolean, reading as 1 for folded polyhedra that can fit into the model fairing and 0 for folded polyhedra that cannot.

Table 14. Fit in Rocket Fairing raw values

{T}	{C}	{O}	{D}	{I}	{RD}	{TP}	{HP}	{TO}	{TI}
0	0	0	0	0	1	0	0	1	1

4. Analysis

4.1 Goal and Obstacles

The goal of this analysis is to determine the overall best-performing shape using the raw values provided by the methodologies described in the evaluation metrics section. There are three obstacles standing in the way of this determination: *performance disconnect*, *dissimilar units*, and *weighting*.

4.1.1 Performance Disconnect

The raw values for each evaluation metric don't necessarily measure the *performance* of each candidate polyhedron. In this case, *performance* refers to how well a given candidate performs compared to the baseline, set by the poorest-performing candidate. The effect of raw values becoming disconnected from the performance is more pronounced for raw values that are large and/or those that are more-tightly grouped to each other. The effect is less-pronounced for an evaluation metric whose poorest-performing (or best-performing) candidate has a value that is close or equal to zero.

4.1.2 Dissimilar Units

The raw values for the various evaluation metrics employ different units that can cause the values to vary greatly in magnitude. Attempting to compare values that can differ by a few magnitudes is akin to comparing grapes to watermelons. The evaluation metrics that produce high magnitude raw values would unduly dominate other evaluation metrics.

4.1.3 Weighting

Not all evaluation metrics should necessarily be weighted the same as all others. While all the evaluation metrics are important, the degree to which they should be accounted for with respect to the others depends on each observer and is therefore subjective to some extent. Conversely, each evaluation metric should not necessarily be weighted as equal by default, as it's highly likely that some metrics are indeed more important than others. Setting bespoke weights for each evaluation metric is valid for an individual decision-maker, but does not necessarily represent the perspective of everyone.

4.2 Methodology

To address the obstacles described in sections 4.1.1-4.1.3, a customized framework for MCDA was employed, where sensitivity analysis was used instead of weight-setting via an expert decision-maker. This process involves the following steps (see also Fig. 13).

1. Transform the raw values into performance values.
2. Normalize the performance values to sum to a total of 1.
3. Using a pre-determined number of levels of importance n_i, generate importance level sets of length equal to the number of candidate polyhedrons c for all combinations of importance levels, resulting in n_i^c importance level sets.
4. Transform the importance level sets into importance factor sets by dividing each element in the importance level sets by the sum of all elements in the importance level set.
5. Remove duplicate importance factor sets.
6. For each unique importance factor set, sum the products of the importance factors and the corresponding raw values for each candidate polyhedron and record the ranking of candidates.
7. The candidate that has the best ranking can be considered most suited for use as a polyhedral space module under most conditions within the number of importance levels analyzed.

The elements described above are described in greater detail in the following briefs.

Raw Values:

The quantitative result obtained when applying the evaluation metric raw value methodology to each candidate polyhedron.

Performance Values:

The values obtained by finding the difference between the raw values and those of the poorest-performing candidate within each evaluation metric;

Copyright ©2023 by Mr. Elliott Ruzicka. Published by the IAF, with permission and released to the IAF to publish in all forms.

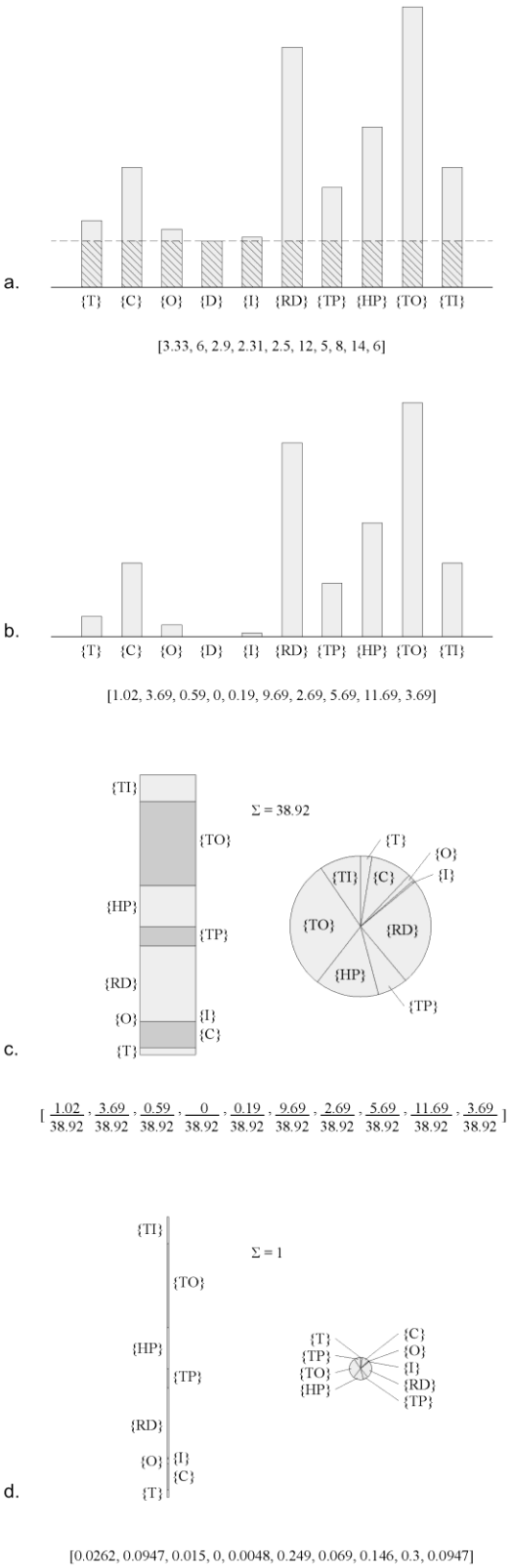

Fig. 13. Normalization of 3.2.11 showing a) raw values and the baseline; b) performance values; c) performance values as parts of a whole; d) normalized values that sum to 1

there will always be at least one performance value within each evaluation metric that is equal to 0.

Normalized Values:

The normalized representation of the performance values obtained by dividing each performance value by the sum of all performance values within the evaluation metric; all performance values within an evaluation metric will sum to 1. This transformation can be described with the following equation:

$$v_n = \frac{v_p}{\sum[v_{p1}, \ldots, v_{p10}]} \quad (4)$$

Importance Levels:

Integers used to assign relative weights to the evaluation metrics. An importance level of 2 represents a weight that is twice that of an importance level of 1 and half as much as an importance level of 4. The higher the number of importance levels, the higher the confidence in the results of the analysis; for example, if only two importance levels are used, a highly important metric can only be weighed twice as high as a less-important metric when the actual difference in importance may be much higher. An importance level set is a list of importance levels wherein each importance level represents an evaluation metric.

Importance Factors:

The normalized representation of the importance levels obtained by dividing the individual importance levels within an importance level set by the sum of importance levels within said set. This process results in an importance factor set. The sum of importance factors in an importance factor set will equal 1.

4.2.1 Application

The normalized values for the candidate polyhedrons were written to a JSON file and a python script was written that generates all combinations of importance levels and systematically sums the products of the resultant importance factors by the normalized values for each polyhedron and records the ranking for each importance factor combination.

The candidate polyhedrons were compared across (14) evaluation metrics using (5) levels of importance. This results in 5^{14} importance level set combinations; however, this figure includes many redundant combinations resulting from sets containing a single number and/or sets comprised entirely of even numbers, which is easily observed after the factorization process. For example, the set {1,1,1,…} and {2,2,2,…} would both produce the same set of importance factors and would, if included in the

Copyright ©2023 by Mr. Elliott Ruzicka. Published by the IAF, with permission and released to the IAF to publish in all forms.

analysis, effectively double-count that combination. Ultimately, the number of unique importance level sets was 6,103,499,239.

5. Results

For the above analysis, the results were clear. Of the 6,103,499,239 combinations of importance level sets, the Rhombic Dodecahedron was not only ranked highest overall, but also remained undominated* in every single one of the combinations analyzed. Table 15 lists these results, showing the average rank, the number of undominated combinations, and the percent of combinations undominated. These results can be replicated using the included raw values tables and the methodology described in section 4.2.

Table 15. Analysis Results

{ }	Name	Rank	#	%
{RD}	Rhombic Dodecahedron	1.00	6,103,499,239	100%
{TO}	Truncated Octahedron	2.63	0	0%
{C}	Cube	2.67	0	0%
{I}	Icosahedron	4.82	0	0%
{D}	Dodecahedron	5.97	0	0%
{TI}	Truncated Icosahedron	6.82	0	0%
{O}	Octahedron	7.01	0	0%
{HP}	Hexagonal Prism	7.21	0	0%
{TP}	Triangular Prism	7.37	0	0%
{T}	Tetrahedron	9.49	0	0%

6. Discussion & Conclusion

6.1 Interpretation of Results

The results of this study are unexpectedly straightforward. Instead of a regular distribution, a singleton has emerged as the only undominated candidate polyhedron. This means that for any combination of (5) importance levels one could place on the included evaluation metrics, the Rhombic Dodecahedron would be indicated as the superior candidate.

The runners up (by average ranking) were the Truncated Octahedron and the Cube, which is unsurprising because they are both lattice-forming and space-filling polyhedra, each balancing their performance in each of the virtue categories listed in section 3.1. The Truncated Icosahedron was ranked 6th out of the (10) polyhedra studied. Despite performing the best in the metrics associated with *simplicity*, the Tetrahedron was the poorest overall performer.

6.2 Limitations

The limitations of this study can largely be considered quantitative limitations, and are discussed in the following sections:

6.2.1 Selection of Candidate Polyhedra

Since the baseline that contributes to the performance values is defined by the performance of specific candidates, the performance values for each evaluation metric could be modified by selecting an alternate set of candidates. It is possible that such an alternate set of candidates could affect the results of the study enough to have an unintended, emergent weighting effect on certain evaluation metrics.

6.2.2 Selection of Evaluation Metrics

While the chosen evaluation metrics are believed to be highly important for discriminating between candidates, other researchers may find them lacking, or that different evaluation metrics should be prioritized. An alternate set of evaluation metrics might have yielded different results.

Additionally, similar to how the number of importance levels was limited, the number of evaluation metrics was set to (14). If fewer or more evaluation metrics were studied, the specific outcome might have again yielded different results.

6.2.3 Evaluation Metric Methodology Decisions

There were two decisions that were made during the methodology formulation process that were necessarily subjective: the 216m^3 notional volume used in sections 3.2.9 and 3.2.14, and the 0.3m notional panel thickness used in sections 3.2.5, 3.2.9, and 3.2.14. These decisions were necessary due to the full-scale nature of the evaluation metrics. It should be noted that these decisions were made prior to evaluation metric methodology application.

The notional volume of 216m^3 was chosen for evaluation metrics that required a full-scale size for analysis. While this size might be considered somewhat arbitrary, this is roughly the volume at which reasonable structural deflection begins to become untenable and the internal layout becomes challenging, requiring added layers of interior partitions and multiple circulation pathways. It is also easy to imagine a cube (6) meters to a side. If this volume were set to an alternative value, different results may have been found, especially for section 3.2.14.

* In the context of MCDA, *undominated* refers to the condition where a certain option is preferred over all other options or otherwise has the best score or ranking.

Copyright ©2023 by Mr. Elliott Ruzicka. Published by the IAF, with permission and released to the IAF to publish in all forms.

The notional volume of 0.3m was chosen as such a thickness should reasonably accommodate the structure required to resist deflection, integrated plumbing and conduit runs, and radiation/impact shielding. This figure may come across as relatively thick compared to contemporary cylinder modules, however this is an unfair comparison. Though Ekblaw assumes the 7.9cm wall thickness of the Columbus Module [6], this thickness was designed for a cylinder, not a flat panel. A flat panel would undoubtedly require much more thickness to resist deflection due to pressurization as well as the various onboard systems.

6.2.4 Number of Importance Levels

For previously described reasons of computational practicality, the number of importance levels adopted in this study was set to (5). This means that any given evaluation metric can only be weighted five times higher than that of the lowest-weighted evaluation metric. If the number of importance levels were set to a higher value, a more robust analysis could be performed that could catch edge cases in situations where a decision maker might weigh one evaluation metric more than five times higher than that of another.

6.3 Implications

Since the findings of this study do not confirm the ongoing direction of research into polyhedral space habitat modules, a reconsideration of foregone conclusions in said research is in order. This study finds that the Truncated Icosahedron in particular is currently overvalued as a viable candidate. While it is understandable that this polyhedron seems intuitively to be an obvious shoo-in due to certain attributes, this does not pass muster once more rigor is applied.

Even if considerations from section 6.2 were used to conduct an alternate study, producing results that were even moderately different from this one, such a study would likely struggle to negate the overwhelming results presented here.

The Rhombic Dodecahedron should be considered the new first choice in candidate selection for polyhedral space habitat modules. Short of this, the Rhombic Dodecahedron should at the very least be given equal consideration to currently researched polyhedra.

6.4 Conclusions

(1) The Rhombic Dodecahedron should be considered the basis-of-design when designing polyhedral space habitat modules.
(2) Deviation from the Rhombic Dodecahedron as the basis-of-design should be accompanied by the selection methodology used as well as ample evidence proving the advantages of such an alternative.
(3) The Truncated Icosahedron should be deprioritized from consideration for polyhedral space habitat module design.

6.5 Final Statement

In his paper, de Weck writes that “the most famous case in nature of hexagonal partitioning are honeycombs…” [3], though that is not completely precise. It would be more precise to say that the volume of the honeycomb cells more closely resembles Rhombic Dodecahedra as it is hexagonal in profile and (3) rhombi can be observed on the back walls of each cell due to the honeycomb cell offset on either side of the honeycomb surface [13] (see also Fig. 14). It is the hope of the author that this fact stands as a testament to the emergent and hitherto unrecognized properties of the Rhombic Dodecahedron and to its future applications in space.

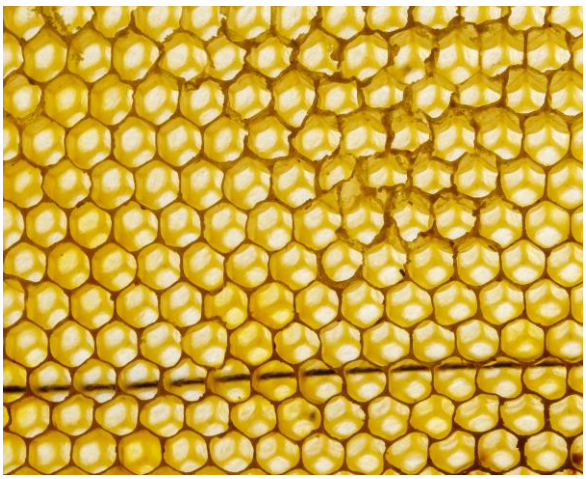

Fig. 14. Honeycomb cells, each having (3) rhombi on the rear of the cell (Image by efe_madrid on Freepik)

Copyright ©2023 by Mr. Elliott Ruzicka. Published by the IAF, with permission and released to the IAF to publish in all forms.

Appendix: Equations

Apothem Length

Name	Equation
Equilateral Triangle	$\ell a = \frac{a}{2\sqrt{3}}$
Square	$\ell a = \frac{a}{2}$
Regular Pentagon	$\ell a = a(\frac{tan(54°)}{2})$
Regular Hexagon	$\ell a = \frac{a\sqrt{3}}{2}$
Rhombus {RD}	$\ell a = a(sin(35.26°))(sin(54.74°))$
Rectangle {TP}	$\ell a = \frac{a}{2} \quad \ell a = \frac{\ell}{2} \quad \ell = \frac{a}{\sqrt{3}}$
Rectangle {HP}	$\ell a = \frac{a}{2} \quad \ell a = \frac{\ell}{2} \quad \ell = a\sqrt{3}$

Volume

{ }	Name	Equation
{T}	Tetrahedron	$V = \frac{a^3}{6\sqrt{2}}$
{C}	Cube	$V = a^3$
{O}	Octahedron	$V = \frac{1}{3}\sqrt{2}a^3$
{D}	Dodecahedron	$V = \frac{1}{4}(15 + 7\sqrt{5})a^3$
{I}	Icosahedron	$V = \frac{5}{12}(3 + \sqrt{5})a^3$
{RD}	Rhombic Dodecahedron	$V = \frac{16\sqrt{3}}{9}a^3$
{TP}	Triangular Prism	$V = \frac{a^2\sqrt{3}}{4}\ell \quad \ell = \frac{a}{\sqrt{3}}$
{HP}	Hexagonal Prism	$V = 3a^2\frac{\sqrt{3}}{2}\ell \quad \ell = a\sqrt{3}$
{TO}	Truncated Octahedron	$V = 8\sqrt{2}a^3$
{TI}	Truncated Icosahedron	$V = \frac{125 + 43\sqrt{5}}{4}a^3$

Surface Area

{ }	Name	Equation
{T}	Tetrahedron	$A_S = \sqrt{3}a^2$
{C}	Cube	$A_S = 6a^2$
{O}	Octahedron	$A_S = 2\sqrt{3}a^2$
{D}	Dodecahedron	$A_S = 3\sqrt{25 + 10\sqrt{5}}a^2$
{I}	Icosahedron	$A_S = 5\sqrt{3}a^2$
{RD}	Rhombic Dodecahedron	$A_S = 8\sqrt{2}a^2$
{TP}	Triangular Prism	$A_S = \frac{a^2\sqrt{3}}{2} + 3a\ell \quad \ell = \frac{a}{\sqrt{3}}$
{HP}	Hexagonal Prism	$A_S = 6a^2\frac{\sqrt{3}}{2} + 6a\ell \quad \ell = a\sqrt{3}$
{TO}	Truncated Octahedron	$A_S = (6 + 12\sqrt{3})a^2$
{TI}	Truncated Icosahedron	$A_S = (20\frac{3}{2}\sqrt{3} + 12\frac{5}{4}\sqrt{1 + \frac{2}{\sqrt{5}}})a^2$

References

[1] W. Frisina, Close-Pack Modules for Manned Space Structures, Journal of Spacecraft and Rockets, 22-5 (1985) 583-584.

[2] W. Frisina, Modular Spacecraft, Journal of Aerospace Engineering, 7-4 (1994) 411-416.

[3] de Weck, W. Nadir, J. Wong, G. Bounova, T. Coffee, Modular Structures for Manned Space Exploration: The Truncated Octahedron as a Building Block, 1st Space Exploration Conference: Continuing the Voyage of Discovery, (2005) p.2764.

[4] A. Ekblaw, J. Paradiso, Self-Assembling Space Structures- buckminsterfullerene sensor nodes, 2018 AIAA SciTech / AHS Adaptive Structures Conference, Smart Assemblies/Systems, Kissimmee, Florida, USA, 2018, 8 - 12 March.

[5] A. Ekblaw, J. Paradiso, Self-Assembling Space Architecture: tessellated shell structures for space habitats, AIAA Scitech 2019 Forum, Smart/Adaptable Deployable Structures, San Diego, California, USA, 2019, 7 - 11 January.

[6] A. Ekblaw, J. Paradiso, Self-Assembling Space Habitats: TESSERAE design and mission architecture, 2019 Ieee Aerospace Conference, Big Sky, MT, USA, 2019, 2 - 9 March.

[7] A. Ekblaw, Space Habitat Reconfigurability TESSERAE platform for self-aware assembly, IAC-19-E5.12, 70th International Astronautical Congress, Washington D.C., USA, 2019, 21 – 25 October.

[8] Ekblaw, A.C. (2020). *Self-Aware Self-Assembly for Space Architecture: Growth Paradigms for In-Space Manufacturing*. PhD diss., Massachusetts Institute of Technology, 2020.

[9] A. Ekblaw, Self-Assembling and Self-Regulating Space Stations- Mission Concepts for Modular, Autonomous Habitats, 2021 50th International Conference on Environmental Systems, 2021, July.

[10] A. Ekblaw, Space Architecture in Microgravity- TESSERAE Project for Large Scale Space Structures, Technology|Architecture + Design, 6:2 (2022) 146-148.

[11] Modularity and Spacecraft Cost, J. Enright, C. Jilla, D. Miller, Modularity and Spacecraft Cost, Journal of Reducing Space Mission Cost. 1 (1998) 133-158.

[12] SpaceX, Falcon User's Guide. September 2021, https://www.spacex.com/media/falcon-users-guide-2021-09.pdf, (accessed 21.08.23).

[13] R. Cardil, Honeycomb, January 2017, http://www.matematicasvisuales.com/english/html/geometry/rhombicdodecahedron/honeycomb.html, (accessed 2023.08.24).